WA07 10:00

Proceedings of the 34th
Conference on Decision & Control
New Orleans, LA - December 1995

Optimal Linear Parameter-Varying Control Design for a Pressurized Water Reactor

Bobby Bodenheimer and Pascale Bendotti
Mail Code 116-81
Dept. of Electrical Engineering
California Institute of Technology
Pasadena, CA 91125

Abstract

The applicability of employing parameter-dependent control to a nuclear pressurized water reactor is investigated. The synthesis technique produces a controller which achieves specified performance against the worst-case time variation of a measurable parameter which enters the plant in a linear fractional manner. The plant can thus have widely varying dynamics over the operating range. The controllers designed perform well over the entire operating range.

Keywords: parameter-dependent control, gain-scheduling, nuclear reactor

1 Introduction

In France and certain other countries the major contribution to electricity production is provided by nuclear power. When this is the case, the nuclear power plant must provide electricity as it is needed, and the plant becomes a time-varying system with dynamics changing slowly as the internal power changes. Nonetheless, large transients can occur, for example, when the plant shuts down. Most nuclear power plants are pressurized water reactors (PWR). The dynamics of a PWR change enough over its operating range that a linear controller cannot guarantee performance over the entire range, especially when operating conditions change suddenly. Indeed, previous work [BenBod94] showed that a fixed linear controller such as an $\mathcal{H}_\infty$ controller cannot maintain performance in the presence of parametric uncertainty corresponding to the change in the operating conditions of the actual plant.

In designing controllers for plants which operate over a wide dynamic range, a common technique is to schedule various fixed-point designs. Unfortunately, there are no known methods for scheduling such controllers which provide an *a priori* guarantee on the resulting performance or stability of the closed-loop system. Additionally, large and often unacceptable transients can occur when switching between controllers. Recent advances in optimal control theory provide a design technique which avoids these difficulties by producing an optimal parameter-dependent controller; i.e., the controller is already scheduled depending on parameter values which are not known beforehand [Pac94, ApkGah94]. The controller is optimized to provide performance against the worst-case time variation of the parameters. Such a controller is called a linear parameter-varying (LPV) controller.

If a fixed linear controller is not capable of maintaining performance over the entire operating range, then a possible approach to control a PWR is to design a parameter-dependent controller with the output power as the parameter. One advantage such a controller would have over a standard gain-scheduled controller is that performance and stability could be guaranteed over the operating range of the plant, and large transients in switching are avoided. An additional advantage of LPV synthesis is that the controller is designed in one step, rather than by designing several controllers and then scheduling them. The potential drawback of LPV synthesis is that the technique is conservative. This conservatism may be so great that the controller performs quite poorly. Our goal in this paper is to determine if LPV synthesis can produce controllers which have reasonable performance, and possibly produce a better control design for the PWR.

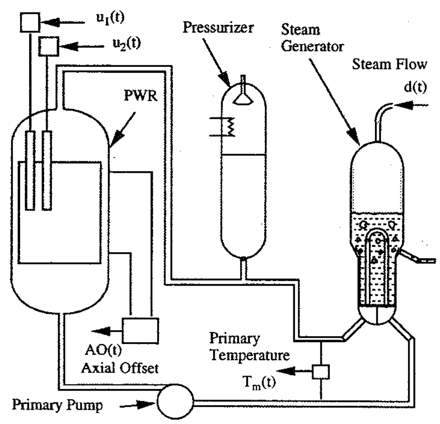

Figure 1: Primary Circuit and Steam Generator.

Section 2 is devoted to the problem statement; in section 3, the model of the PWR as it pertains to LPV design is discussed. Section 4 overviews the synthesis theory, and the structure for controller design on the PWR; the behavior of these controllers is examined in section 5. Our conclusions and some directions for future work end the paper.

2 Problem Statement

The main objective in controlling a PWR is to provide the commanded power while respecting certain physical constraints. Consider the application depicted in Figure 1. This is the primary circuit, and our goal is to control this part of the reactor. The pressurized water in the primary circuit transmits the heat generated by the nuclear reaction to the steam generator. In the steam generator, water of the secondary circuit turns into hot steam, which drives a turbo-alternator to generate electricity. The rate of the reaction is regulated by the control rods. The rods capture neutrons, slowing down the nuclear reaction; withdrawing them increases the reaction. The PWR has two independent sets of rods which are used as controls.

The PWR has an inner control loop which holds the pressure in the primary circuit constant. Thus for a steam flow increase in the secondary circuit, the temperature in the primary circuit will decrease. From a control standpoint, the required power corresponds to a specific steam flow that may be viewed as a measurable disturbance. Hence, one natural control objective is to track a temperature reference derived from the steam flow. Because of the way in which the control rods enter the reactor, the rate of reaction is always higher at the bottom of the reactor. The *axial offset* is defined as the difference in power generated between the top and bottom of the PWR. Safety specifications require minimizing the axial offset; this also increases the lifetime of the fuel and reduces operating

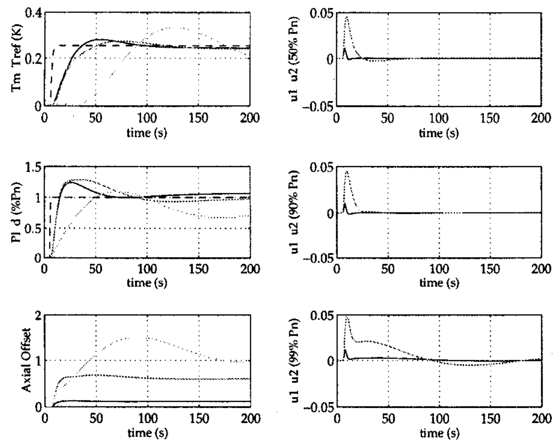

Figure 2: Closed-loop responses of an $\mathcal{H}_\infty$ controller with linearized models of the PWR at $0.5\mathcal{P}_n$ (solid), $0.9\mathcal{P}_n$ (dark), and $0.99\mathcal{P}_n$ (light).

costs. To achieve such objectives two control inputs are available, the rates of motion of the control rods, denoted u_1 and u_2. The positions of the control rods are denoted v_1 and v_2, respectively. The positions are, of course, measurable. Due to the physics of the reactor, u_2 has more authority than u_1 at low power, and using it results in a smaller axial offset. At high power, however, u_2 has almost no authority, so all control must come from u_1.

Due to the complexity of the physical plant, performance specifications cannot be uniquely or easily derived. Indeed, investigations into the best performance specifications are currently underway at Electricité de France (EDF). In [BenBod94], we made the first attempt to automatically control the axial offset, a specification we will also use here. Nonetheless, we do not have precise specifications the controllers must meet.

Previously, the authors designed an $\mathcal{H}_\infty$ controller using a linear model of the plant identified at 50% of the nominal power, $\mathcal{P}_n$ [BenBod94]. In addition to actuator dynamics and modelling error, the uncertainty description covered the variations in dynamics of the plant depending on power with time-invariant uncertainty. This controller performs satisfactorily up to $0.9\mathcal{P}_n$, but not at $0.99\mathcal{P}_n$. Figure 2 shows the step-responses of the closed-loop systems. T_m is the mean temperature of the plant, and T_{ref} (dashed lines) is the reference signal. P_l is the primary power $\mathcal{P}$, and d (dashed lines) is the steam flow input. Input-output signals corresponding to the nominal model are plotted in solid lines while those resulting from the perturbed models corresponding to $0.9\mathcal{P}_n$ and $0.99\mathcal{P}_n$ are displayed in dark and light shaded lines, respectively. The control signals are plotted in dark (u_1) and light (u_2) shaded lines. The above suggests that a linear controller is not enough to ensure performance over the entire operating range.

3 Modeling

The synthesis technique for designing a parameter-dependent controller requires a model which has accurate dynamics over the operating range of interest. A general time-varying system is shown pictorially in Figure 3, where $x(k), e(k), y(k), w(k)$, and $u(k)$ are the state, error, measurement, disturbance and input vectors, respectively. We assume the time-variation of the plant can be represented as a linear-fractional transformation (LFT) of a parameter and a constant matrix. Thus $P(k)$ is given by

$$P(k) = P_{22} + P_{21}\Delta(k)\,(I - P_{11}\Delta(k))^{-1}P_{12} \tag{1}$$

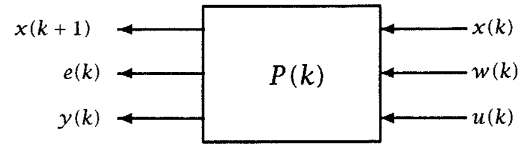

Figure 3: Time-Varying System.

where

$$\Delta(k) = \begin{bmatrix} \delta_1(k)I_{n_1} & & \\ & \ddots & \\ & & \delta_m(k)I_{n_m} \end{bmatrix} \tag{2}$$

with $|\delta_i(k)| \le 1$ for all k. The δ_i are assumed to be measurable. Any rational time-varying system can be represented in this framework, and many others can be arbitrarily closely approximated. This type of system is known as a parameter-dependent LFT system.

Previous work on the PWR ([BenIrv93]) identified three sixth-order linear models which characterize the behavior around $0.5\mathcal{P}_n$, $0.9\mathcal{P}_n$, and $0.99\mathcal{P}_n$. These models were identified using a realistic non-linear simulator of the PWR developed by EDF. As described in [BenBod94] the models can be reduced quite accurately to first-order models using frequency-weighted balanced truncation. Our model in the form of Equation 1 will be derived using these first-order models.

To derive the parameter dependence, each term of the three first-order models is compared; those which vary are individually fitted with a rational function of δ, $-1 \le \delta \le 1$, using a least-squares technique. For the PWR, first order LFTs of the form $e + f\delta(1 - g\delta)^{-1}h$ fit the parameters extremely well, as shown in Figure 4. In this figure, $0.5\mathcal{P}_n$ corresponds to $\delta = -1$, $0.9\mathcal{P}_n$ corresponds to $\delta = 0.6$, and $0.99\mathcal{P}_n$ to $\delta = 0.998$ (these are the asterisks in the figure). The resulting model with δ-dependence, $P(\delta)$, becomes

$$\begin{bmatrix} A & B \\ C & D \end{bmatrix} = \begin{bmatrix} a(\delta) & b_1 & b_{v_1}(\delta) & b_{v_2}(\delta) \\ c_1 & d_{11} & d_{12} & d_{Tm_2}(\delta) \\ c_2 & d_{12} & d_{22} & \kappa b_{v_2}(\delta) \\ c_{AO}(\delta) & 0 & d_{AO_1}(\delta) & d_{33} \end{bmatrix} \tag{3}$$

The inputs for this model are the steam disturbance d, v_1, and v_2; the outputs are the mean temperature T_m, the power $\mathcal{P}$, and the axial offset AO, respectively (see Figure 1). Placing this model in the form of Equation 1 results in a system shown in Figure 5, where $n_0 = 1$ and $\Delta = [\delta I_{6\times6}]$.

From Figure 4, notice the system matrix $a(\delta)$ is inversely proportional to the operating power, and the time constant changes by a factor of 2 over the operating range. Also, the variation of b_{v_2} and d_{P_2} differs only by a constant, κ, which is used to reduce the size of the final Δ-block. More importantly, the effectiveness of u_2 decreases as the power increases, and is almost zero at full power. The gain in the axial offset channel increases as power increases, making it more difficult to control at high power. In particular, the effect of u_1 on the axial offset (d_{AO_1}) increases, while the effect of u_2 is decreasing. This makes it practically impossible to require any performance on axial offset at high power.

4 Synthesis

In this section a brief overview of the synthesis theory is presented. Since our intent is to convey only a general understanding of the theory, we will be somewhat loose in our notation. A complete and rigorous explanation of the synthesis technique can be found in [Pac94].

From the previous section, the plant has the structure given in Figure 5. The controller we will design for this plant will also be parameter-dependent, depending on the same measurable δ_i's as the plant; these copies are collectively denoted by $\hat{\Delta}$. K thus has the form shown in Figure 6. P can be augmented to collect all the time-varying parameters and states

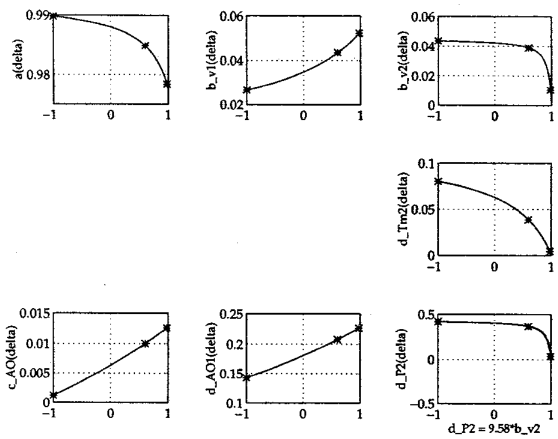

Figure 4: Parameter Variations versus δ for the model of Equation 3. A '*' shows an actual value, and the line shows the LFT fit.

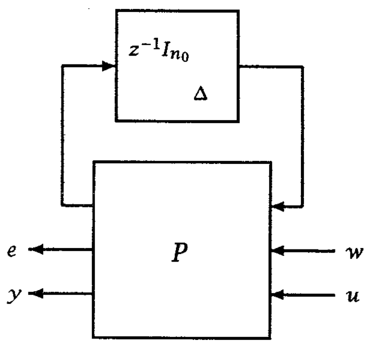

Figure 5: Parameter-Dependent Plant. The $z^{-1}I_{n_0}$ term represents the states of P, and the Δ represents the time variation of Equation 2.

together; K can then be treated as a simple matrix. This is depicted in Figure 7, where R is the augmented form of P, and K is a matrix. The problem thus appears as a robust control problem with a special structure on the plant and parameters. The design objective is to find a controller K such that the interconnection is stable and the $\ell_2 \to \ell_2$ induced norm from w to e is small for all allowable parameter variations $\Delta(k)$ (see Equation 2). This is simply a small-gain condition. Since the small-gain theorem can be quite conservative, we can reduce the conservatism by introducing scaling matrices from a set $\mathcal{D}$ which commutes with the set of parameter variations.

The resulting condition is then the state-space upper bound (SSUB) of [PacDoy93]. Introducing the notation $\mathcal{F}_l(R,Q) = R_{11}+R_{12}Q(I-R_{22}Q)^{-1}R_{21}$ for a block partitioned 2×2 matrix R with $\det(I-R_{22}Q) \neq 0$, this condition becomes (compare Lemma 3.1 of [Pac94] and Theorem 10.4 of [PacDoy93]):

Theorem 1 *Let R be given as above, along with an uncertainty structure Δ. If there is a $D \in \mathcal{D}$ and a stabilizing, finite-dimensional, time-invariant K such that*

$$\left\| \begin{bmatrix} D & 0 \\ 0 & I \end{bmatrix} \mathcal{F}_l(R,K) \begin{bmatrix} D^{-1} & 0 \\ 0 & I \end{bmatrix} \right\|_\infty < 1 \qquad (4)$$

then there is a γ, $0 \leq \gamma < 1$, such that for all parameter sequences $\delta_i(k)$ with $\|\delta_i\|_\infty \leq 1$, the system in Figure 7 is internally exponentially stable, and for zero initial conditions, if $w \in \ell_2$, then $\|e\|_2 \leq \gamma \|w\|_2$.

Pictorially, this theorem is shown in Figure 8. The important fact about Theorem 1 is that the synthesis of D and K to meet the objective can be cast as a computationally tractable convex optimization problem involving 3 LMIs. These LMIs have the

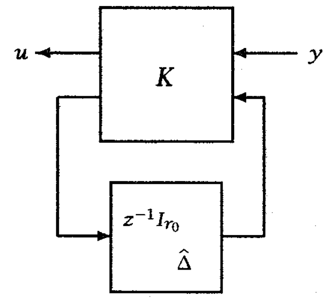

Figure 6: Parameter-Dependent Controller; $z^{-1}I_{r_0}$ represents the states of the controller and $\hat{\Delta}$ the time variations.

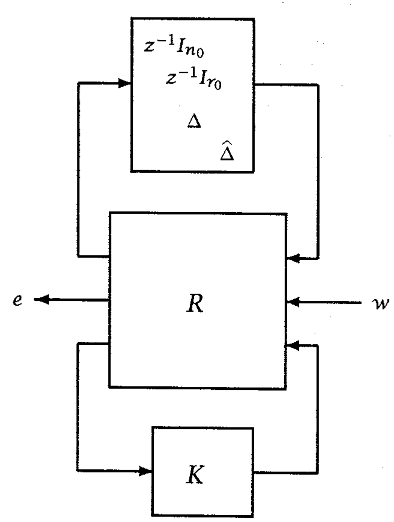

Figure 7: Parameter-Dependent Closed-Loop System.

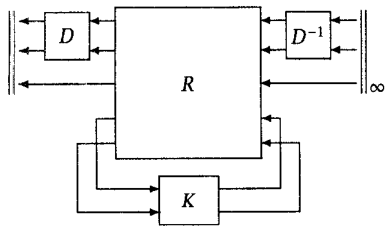

Figure 8: Diagram of Theorem 1.

following form:

$$U_\perp^T\left(E\begin{bmatrix} X & 0 \\ 0 & I \end{bmatrix}E^T-\begin{bmatrix} X & 0 \\ 0 & I \end{bmatrix}\right)U_\perp<0$$

$$V\left(E^T\begin{bmatrix} Y & 0 \\ 0 & I \end{bmatrix}E-\begin{bmatrix} Y & 0 \\ 0 & I \end{bmatrix}\right)V^T<0$$

$$\begin{bmatrix} X & I \\ I & Y \end{bmatrix}\geq 0$$

where $U_\perp$, $V_\perp$, and E are obtained from the system realization, and X and Y are structured positive definite matrices. Interested readers may find the exact LMIs in Theorem 6.3 of Packard [Pac94]. E, U, and V have a scaling γ absorbed into them, and thus the synthesis procedure is a γ-iteration, as $\mathcal{H}_\infty$ is. Once a desired γ level has been reached, a controller K can be obtained by linear algebraic operations on X and Y.

A few points are important in understanding the ramifications of employing the state-space upper bound (SSUB). Most importantly, this technique results in a controller optimal with respect to a time-varying perturbation with memory (the sequence $\Delta(k)$ of Equation 2, becomes a time-varying operator with memory, rather than a sequence of complex numbers). The relationship between such an operator and a parameter useful in gain-scheduling is tenuous, at best. Depending on the problem, this technique could conceivably yield controllers so conservative as to have extremely poor performance. Nonetheless, if a controller with acceptable performance can be designed with this technique, then it will have at least the same level of performance for all variations of the operating point (the operating point is a fixed value of Δ). Additionally, a time-varying operator with memory does not in general have a frequency spectrum, so there is no way to "filter" it to achieve a closer relationship to an operating parameter. Moreover, it is interesting to contrast this technique with μ-synthesis where instead of the SSUB the frequency-domain upper bound is usually employed; this difference reflects the different assumptions about the type of perturbations.

4.1 Controller Design

Once the parameterized model $P(\delta)$ is obtained, the controller design becomes similar to an $\mathcal{H}_\infty$ design. Both LPV and $\mathcal{H}_\infty$ synthesis produce controllers which reject disturbances. A tracking problem, such as the PWR, can be cast in this framework by rejecting the low frequency components of the error between the plant output and the reference. The tracking will become faster as higher frequencies are rejected. The synthesis structure used is shown in Figure 9, with uncertainty and performance weights included. In particular, w_{ref}, w_d, and w_n are weighted reference, disturbance, and noise signals, respectively.

W_m is a multiplicative uncertainty weight covering unmodelled dynamics, error introduced by model reduction, and modelling errors as the plant changes operating point. The performance weight W_p is a diagonal matrix

$$W_p=\begin{pmatrix} W_{T_m} & & & \\ & W_{P_I} & & \\ & & W_{AO} & \\ & & & W_{pos} \end{pmatrix} \tag{5}$$

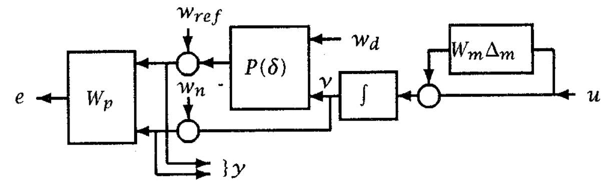

Figure 9: Synthesis structure for the PWR.

which weights the performance on temperature, power, axial offset, and vertical position of the control rods. To insure low steady-state error in tracking, W_{T_m} resembles an integrator. These weights can depend on δ as well, so, ideally, high performance could be required at one operating point and lower performance at another. Nevertheless, since a δ in the weight adds another time-varying perturbation with memory, it may be that performance is degraded instead.

Two controllers were designed. The first is called "LPV #1" and is an LPV controller with weights similar to the weights employed for the $\mathcal{H}_\infty$ controllers of Figure 2. The second is called "LPV #2" and uses the same weights as LPV #1, except W_{AO} was allowed to depend on δ. W_{AO} was designed to require high performance in axial offset for $\delta \approx -1$, but less performance as $\delta \to 1$.

5 Results

The LPV controllers will be compared with $\mathcal{H}_\infty$ controllers designed for the plant models at $0.5\mathcal{P}_n$ and $0.99\mathcal{P}_n$. The controller designed at $0.5\mathcal{P}_n$ will be called "H50" and the one at $0.99\mathcal{P}_n$ "H99."

Figure 10 shows the step responses of the closed-loop systems consisting of each of the controllers and a linearization of the plant at $0.99\mathcal{P}_n$. Step responses are shown because we are interested in the low frequency rejection properties of the closed-loop system. In the first column of plots, the dashed lines are the reference signals; the solid lines are the responses with the first LPV controller; the light shaded lines are with the second LPV controller; the dark shaded lines are with H99. The second column of plots shows u_1 and u_2 for each of the controllers; u_1 is the solid line and u_2 the shaded one. Figure 11 is identical to Figure 10, except the responses are with respect to a linearization of the plant at $0.5\mathcal{P}_n$.

Because the control rods are almost withdrawn from the reactor at high power, the plant is more difficult to control. Referring to Figure 10, the LPV controllers are almost identical in behavior. They perform equally well, but are not as fast as H99, although they have no overshoot on the temperature. The noticeable difference is that the LPV controllers have less axial offset than H99. At this power, we consider LPV #2 the best of these controllers.

Some of this behavior is preserved in Figure 11, but the model is quite different here. Here H50 is slightly faster than the LPV controllers. The major difference at this power is that u_2 has more control authority at this power, so controllers do better to use it more than u_1, since this results in lower axial offset. H50 does use it more, and the axial offset is considerably lower. At this operating point, we consider H50 the best controller.

At low power, u_2 is the dominant control, but as the power increases u_1 should be used more and more to better meet the control objectives. The LPV controllers do not change strategy between these operating points. Notice that the control plots for LPV #2 are almost identical, up to a scale change in magnitude. This is probably a result of the worst-case nature of LPV controllers. Since achieving worst-case performance does not require a change of strategy, and may in fact forbid one, the controllers do not change their use of the inputs.

Next, the behavior of the LPV controllers on a nonlinear simulator of the PWR is shown. EDF would not allow the

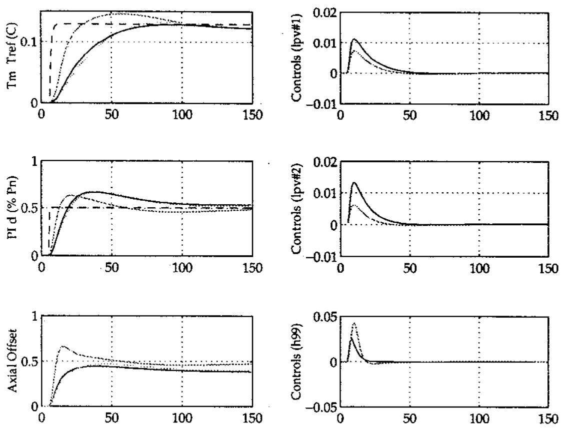

Figure 10: Comparison of Three Controllers at $0.99\mathcal{P}_n$.

use of the nonlinear simulator used previously for identification [BenBod94] and thus a nonlinear simulator based on first principles models was used. This simulator is not the simulator the synthesis model was identified from, and has less accurate dynamics. Nonetheless, the one used is reasonably accurate and provides a satisfactory way to simulate the behavior of the closed loop system. The simulator includes models for the pressurizer, steam generator, and turbine, but not the alternator. The largest underlying change between the simulator used for identification and the simulator used for evaluation is that the former simulator was used assuming the nuclear fuel was new, while the latter is configured for nuclear fuel which is at half its expected lifetime. In particular, as the fuel ages it becomes less active, and thus control authority is increased.

Figures 12 through 14 show the simulation results. In these figures, the response of LPV#1 is shown in shaded lines, the response of LPV#2 is shown in solid lines, and the references are shown in dashed lines. Also, u_1 is shown in shaded lines, and u_2 in solid lines. Figure 12 shows the response to a one percent step around $0.99\mathcal{P}_n$. LPV#2 is faster, and introduces less axial offset. This difference is even more noticeable in Figure 13, which is a two percent step around $0.5\mathcal{P}_n$. Comparing these results to the linear simulations, there is overshoot and the response is slower. LPV#2 clearly outperforms LPV#1 in the nonlinear simulations.

Finally, the response of the LPV controllers to a large transient is shown in Figure 14. This is a ramp of -30%/minute from $\mathcal{P}_n$ to $0.5\mathcal{P}_n$. There is not much difference in either LPV controller on this trajectory. This is not surprising, as stability for large transients is inherent in the LPV methodology, provided that the synthesis model is accurate over the operating range.

6 Conclusion

In this paper we investigated using an LPV controller to control a PWR. The controllers were simulated first on a linear simulation and then on a complete nonlinear simulation with both small changes and large transients. The controllers performed well, especially LPV#2, and this demonstrates that the LPV design methodology is applicable to a realistic complex system. Our result is particularly interesting since the dynamics of the PWR change slowly, but the LPV synthesis is a worst-case time-varying design. The prejudice against applying this technique is that worst-case time variations are "fast", and thus controllers with low performance would result. The LPV controllers compared favorably with linear controllers on a linear simulation. On the nonlinear simulation, the LPV controllers performed well even for small operating changes, where the assumptions on the uncertainty are extremely conservative.

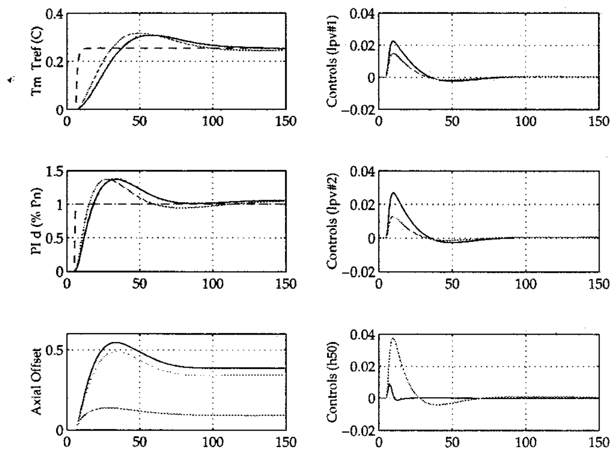

Figure 11: Comparison of Three Controllers at $0.5\mathcal{P}_n$.

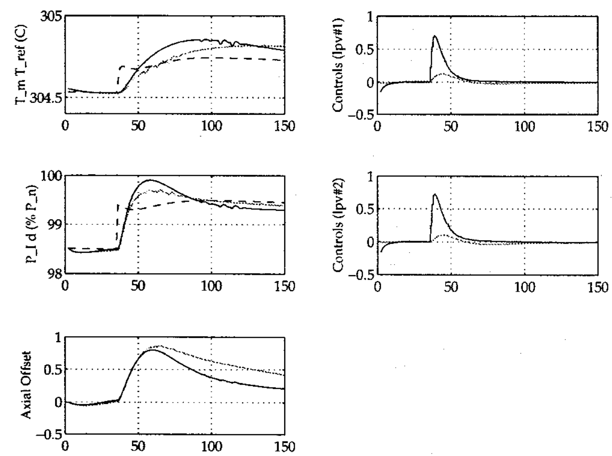

Figure 12: Comparison of LPV Controllers on a Nonlinear Simulation to a Step Around $0.99\mathcal{P}_n$.

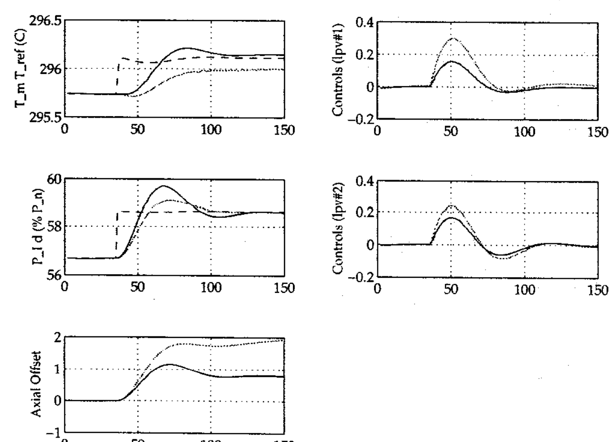

Figure 13: Comparison of LPV Controllers on a Nonlinear Simulation to a Step Around $0.5\mathcal{P}_n$.

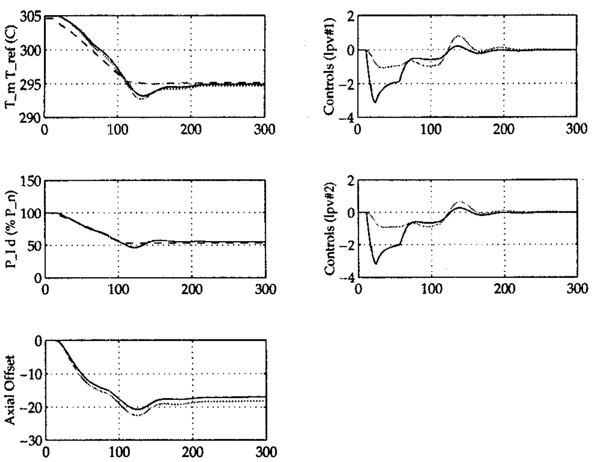

Figure 14: Comparison of LPV Controllers on a Nonlinear Simulation to a Large Transient.

We have not presented a complete controller design for the primary circuit of the PWR. A complete control system would, for example, account for saturation nonlinearities in the input signals, and usually has a dead-band built-in to minimize the movement of control rods to small variations in operating conditions. Accounting for saturations to prevent wind-up is certainly an essential component of any realistic design, and will be considered in our future efforts towards design of a complete system. Our next goal is to re-examine the temperature reference to determine if a reference derived differently leads to better minimization of the axial offset.

An advantage of the LPV designs over conventional methods of gain scheduling is they design a controller of fixed order that works reasonably for all plants in the operating regime. Their major drawback for the PWR is they do not switch control strategy between low and high power. This is perhaps attributable to the worst-case nature of the designs, but methods are now being investigated which attempt to alleviate this problem without losing the performance guarantees.

Additionally in this paper, we demonstrated that parameter variations can be placed in weights with beneficial effect. This is the first time a design has been tried using this technique, and it is important because for many systems, one can expect dynamics to change so much that "frozen" time-invariant specifications will not yield adequate performance. This type of problem arises even in adaptive control.

A further question to explore is whether the size of the time-varying parameter block (in the case of $P(\delta)$, 6) is a significant factor limiting the performance. $P(\delta)$ could be reduced and controllers designed for the reduced-order plant. Do they work and achieve significantly better performance? One way of checking whether the plant is reducible in the size of the Δ-block is to treat the state as an input and output, and the Δ-block as the state, then look at the Hankel singular values of the system. For the PWR they are: 2.5448, 0.1031, 0.0325, 0.0187, 0.0152, and 0.0035. This indicates the size of the Δ-block could probably be reduced by at least one. A more sophisticated method is found in [Beck94], where the state is included in the reduction, i.e., true multidimensional model reduction. This technique provides reduction of the uncertainty description in a manner similar to balanced truncation model reduction. Preliminary results with this also indicate a reduction of one is quite reasonable.

Acknowledgements

The authors thank Jorge Tierno for many helpful discussions. Richard Murray, John Doyle, and Carolyn Beck provided useful comments. The second author gratefully acknowledges financial support provided by Ministère de la Recherche et de l'Espace (MRE), France.

References

[BenBod94] Bendotti, P., and B. Bodenheimer, "Identification and $\mathcal{H}_\infty$ Control Design for a Pressurized Water Reactor", *Proc. of the 33rd IEEE Conf. on Decision and Control*, FL, 1994.

[BenIrv93] Bendotti, P. and E. Irving, "Modeling and Robust Frequency-shaped LQG Control of a Pressurized Water Reactor", *Internal Note, EDF HI/20/93/009*, August 1993.

[Pac94] Packard, A., "Gain Scheduling via Linear Fractional Transformations", *Systems and Control Letters*, v. 22, Feb. 1994, pp. 79-92.

[ApkGah94] Apkarian P. and P. Gahinet, "A Convex Characterization of Parameter Dependent $\mathcal{H}_\infty$ Controllers", submitted to *IEEE Trans. on Automatic Control.*

[PacDoy93] Packard, A., and J. Doyle, "The Complex Structured Singular Value", *Automatica*, Vol. 29, No. 1, 1993, pp. 71-109.

[Beck94] Beck, C., "Minimality for Uncertain Systems and IQCs", *Proc. of the 33rd IEEE Conf. on Decision and Control*, FL, 1994.